Active and Passive Surface Wave Measurements at the William Street Park Site, Using F-K Methods

By Sungsoo Yoon[1] and Glenn J. Rix [2]

This paper is an extract from

Asten, M.W., and Boore, D.M., eds., Blind comparisons of shear-wave velocities at closely spaced sites in San Jose, California: U.S. Geological Survey Open-File Report 2005-1169. [available on the World Wide Web at http://pubs.usgs.gov/of/2005/1169/].

2005

U.S. DEPARTMENT OF THE INTERIOR
U.S. GEOLOGICAL SURVEY

[1]Graduate Research Assistant

[2] Associate Professor of Civil and Environmental Engineering,
School of Civil and Environmental Engineering

Georgia Institute of Technology

Surface wave measurements were performed at the Williams Street Park site near the intersection of 16th Street and Williams Street in San Jose, California on July 8, 2003 to measure the shear wave velocity (V_S) profile. An active surface wave test was performed using a harmonic source and an irregular linear array of receivers as shown in Figure 1. Since the site contained a large flat area and was surrounded by excellent passive sources from downtown San Jose, Interstate Highway 280, the Pacific Ocean, and San Francisco Bay, nine passive surface wave tests were successfully performed using three different circular arrays of receivers. A mixture of Kinemetrics SS-1 Rangers, shown in Figure 2(a), and Mark Products L4-C, shown in Figure 2(b), geophones was used as receivers.

Figure 3 shows the general configuration of the source, receivers, and recording equipment in the active test. The source generated surface (Rayleigh) waves at 54 frequencies ranging from 4 to 100 Hz that were monitored by a linear array of 15 receivers at distances ranging from 2.4 to 33.5 m (8 to 110 ft) from the source. There is a trade off between spatial aliasing and spatial resolution for a given number of receivers. An irregular linear array of receivers spaced at 2.4, 3, 3.7, 4.6, 5.5, 6.7, 8.5, 10.4, 12.8, 15.2, 18.3, 21.3, 24.4, 29, and 33.5 m was selected to optimize the array geometry considering spatial aliasing and spatial resolution with the given number of receivers (15) and maximum cable length (35 m) (Zywicki, 1999).

In addition to the active test, the nine passive tests were performed using 16-receiver circular arrays with the radii of 30, 40, and 50 meters to allow deeper V_S profiling. The receivers were equally spaced along the circumference of the circular array. During each passive test, passive energy was collected for 256 seconds at a sampling frequency of 320 Hz. The 2^{16} time domain records in each passive test were divided into 16 blocks to average them in frequency domain to reduce the variance of the signal. The frequency resolution in the passive tests was: $\Delta f = f_S/N = 320/4096 = 0.078$ Hz.

In both tests, time histories recorded at each receiver were used to calculate the surface wave phase velocities using the frequency-wavenumber (*f-k*) method (Rix et al., 2002). In the *f-k* method, k_{peak} is the wavenumber of propagating Rayleigh waves corresponding to a peak value in a steered response power spectrum. For a frequency f_0, the Rayleigh wave phase velocity is calculated using:

$$V_R = \frac{2\pi f_0}{|k_{peak}|} \quad (1)$$

The value of the wavenumber associated with each peak k_{peak} is a vector quantity in the passive tests, whereas it is a scalar value in the active tests. For further details on the *f-k* method used in this study, refer to Rix et al. (2002).

The experimental dispersion curve from the active test at the Williams Street Park site is shown in Figure 4. Figure 5 shows the frequency content of the passive energy at the Williams Street Park site, which is concentrated at low frequencies ranging from about 2 to 10 Hz. With the maximum wavenumber and the wavenumber resolution determined by the minimum distance between adjacent receivers and the total sampling distance used in the tests, dispersion data ranging from about 2 to 8 Hz were obtained from the passive tests as shown in Figure 6. Figure 6 shows experimental dispersion curves from the nine passive tests and a representative experimental dispersion curve that is obtained by averaging them. The active and averaged passive dispersion curves at the Williams Street Park site are combined to form a composite dispersion curve as shown in Figure 7. The curves overlap from approximately 4 to 8 Hz and there are differences between them as shown in the figure inset. These differences, which decrease with increasing frequency, are likely due to "near-field" effects.

In surface wave methods, it is usually assumed that only plane Rayleigh waves are measured during testing. The region where the assumption is no longer valid is called the near-field, and any error resulting from the invalid assumption is called a near-field effect. Two main causes of near-field effects are body wave interference and model incompatibility. Body wave interference is a well-known cause of near-field effects. Since the amplitude of body waves decreases more rapidly with distance from an active source than Rayleigh waves, the interference becomes smaller as the distance increases. Furthermore, it is recognized that the interference becomes smaller with increasing frequency because higher frequency body waves are attenuated more and thus the measurements of pure Rayleigh waves are influenced less. The model incompatibility arises from estimating phase velocities for cylindrically spreading surface waves with a plane wave model, causing errors that decrease with increasing frequency (Zywicki, 1999b). It is noteworthy that both causes result in near-field effects that become more severe as frequency decreases, i.e., wavelength increases. In this study, a composite dispersion curve was obtained by using only the passive dispersion curve within the range of overlapping frequencies. Assuming only plane Rayleigh waves are measured in the passive tests, this method of combining the active and passive dispersion curves should provide a composite dispersion curve containing fewer near-field effects.

The shear wave velocity profile is subsequently determined from the experimental dispersion curve via a process called inversion. A non-linear, constrained least squares inversion algorithm (Lai, 1998) was used in this study. A brief summary regarding the inversion algorithm used in this report is described in Rix et al. (2002). For an inversion using only the active dispersion curve, the theoretical dispersion curve corresponding to the shear wave velocity profile at the Williams Street Park site is obtained and shown in Figure 8. The good agreement between experimental and theoretical dispersion curves is indicative of a successful inversion. The shear wave velocity profile obtained from the active test is shown in Figure 10 and listed in Table 1. An estimated uncertainty in shear wave velocity of each layer is calculated using Equation (2) and is also shown as a horizontal bar in Figure 10.

$$Cov(V_s) \approx [(\mu\partial^T\partial + (W_{V_R}J_S)^T W_{V_R}J_S)^{-1}(W_{V_R}J_S)^T W_{V_R}] \cdot \tag{2}$$

$$Cov(V_R) \cdot [(\mu \partial^T \partial + (W_{V_R} J_S)^T W_{V_R} J_S)^{-1} (W_{V_R} J_S)^T W_{V_R}]^T$$

where μ is the Lagrange multiplier, which may be interpreted as a smoothing parameter, ∂ is an *nl* × *nl* real-valued matrix that defines the two-point finite difference operator, *W*is an *nf* × *nf* diagonal matrix defined by $W = \text{diag}\{1/(\sigma)^{V_R V_R V_R}{}_1, 1/(\sigma)^{V_R}{}_2, \ldots, 1/(\sigma)^{V_R}{}_{nf}\}$, J_S is an *nf* × *nl* Jacobian matrix whose elements are the partial derivatives of the Rayleigh phase velocities with respect to the shear wave velocities of the layers ($\partial V_R / \partial V_S$), *nl* is the number of layers, and *nf* is the number of frequencies. The value σis the standard deviation associated with the experimental data and was assumed equal to 5% of the value of $V^{V_R}{}_R$. For a detailed description of the terms used in Equation (2), refer to Lai (1998).

A second inversion was performed using the composite dispersion curve as shown in Figure 9 to obtain a shear wave velocity profile at greater depth. The shear wave velocity profile corresponding to the composite dispersion curve with the estimated uncertainties is shown in Figure 11 and listed in Table 2. Figure 12 shows the comparison of shear wave velocity profiles corresponding to the active and the composite dispersion curves. Adding the passive data to the active data increases the maximum depth from 30 m to 130 m as shown in Figure 12. Rayleigh wave velocities in the composite dispersion curve are greater than those in the active dispersion curve over the range of frequencies where they overlap as shown in Figure 7. Consequently, higher shear wave velocities were obtained from the composite dispersion curve compared to those from the active test at depths between 10 ~ 30 m as shown in Figure 12. Slight differences were observed in the average shear wave velocities in the upper 30 m from the active and composite dispersion curves as listed in Tables 1 and 2.

Although it is possible to obtain a shear wave velocity profile to approximately 30 m using the active dispersion curve, it should be noted that the shear wave velocities may be underestimated due to near-field effects. If passive tests are feasible, the combination of active and passive measurements may help to mitigate near-field effects as well as provide a shear wave velocity profile to greater depth.

References

Lai, C. G. (1998), "Simultaneous Inversion of Rayleigh Phase Velocity and Attenuation for Near-Surface Site Characterization", Ph.D. Dissertation, Georgia Institute of Technology, pp.370.

Rix, G. J., Hebeler, G. L., and Orozco, M. C. (2002), "Near-Surface V_s Profiling in the New Madrid Seismic Zone Using Surface Wave Methods", *Seismological Research Letters*, 73(3), 380-392.

Zywicki, D. J. (1999), "Advanced Signal Processing Methods Applied to Engineering Analysis of Seismic Surface Waves", Ph.D. Dissertation, Georgia Institute of Technology, pp. 228.

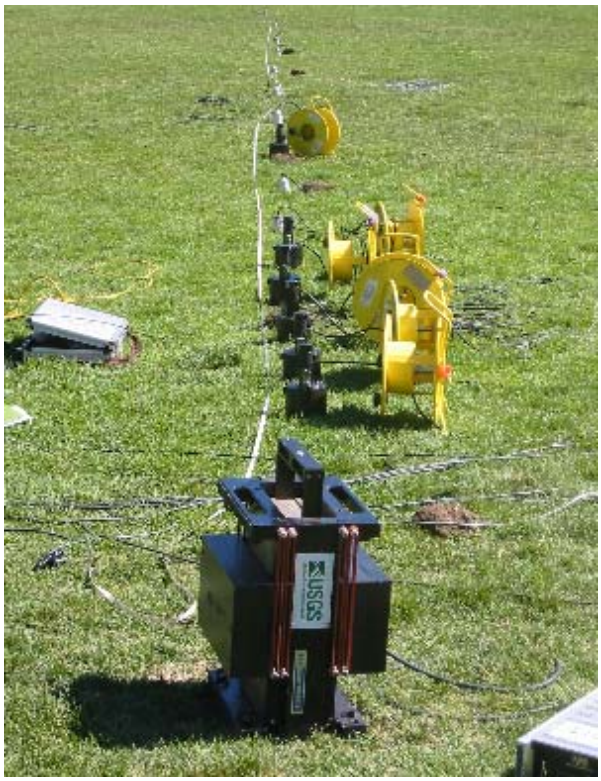

Figure 1. Placement of a harmonic source and receivers in an active test

(a) (b)

Figure 2. Receivers used in both active and passive tests: (a) Kinemetrics SS-1 Ranger geophone, and (b) Mark Products L4-C geophone

Figure 3. Source-receivers configuration used for active surface wave testing

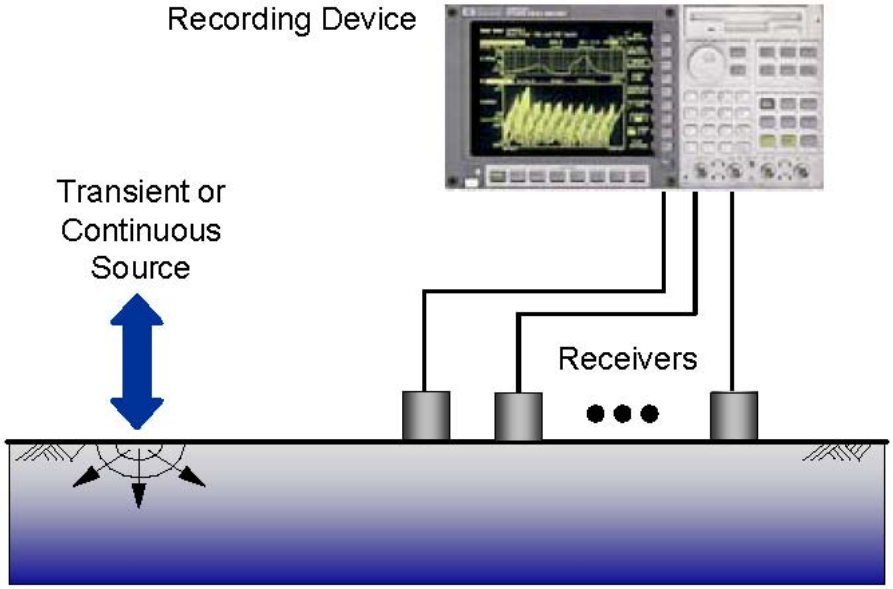

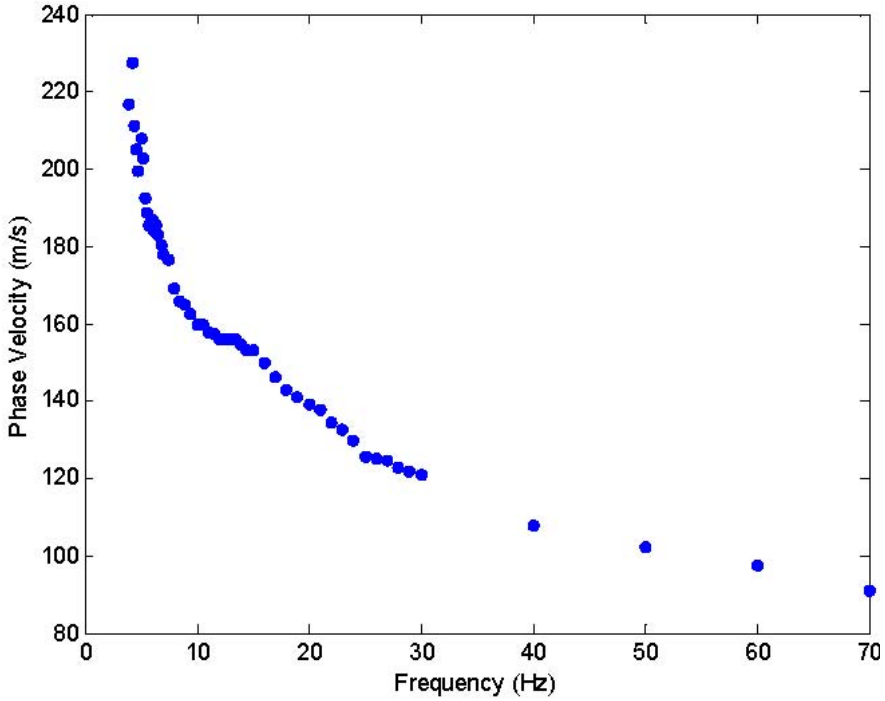

Figure 4. Experimental dispersion curve at the Williams Street Park site (Active test)

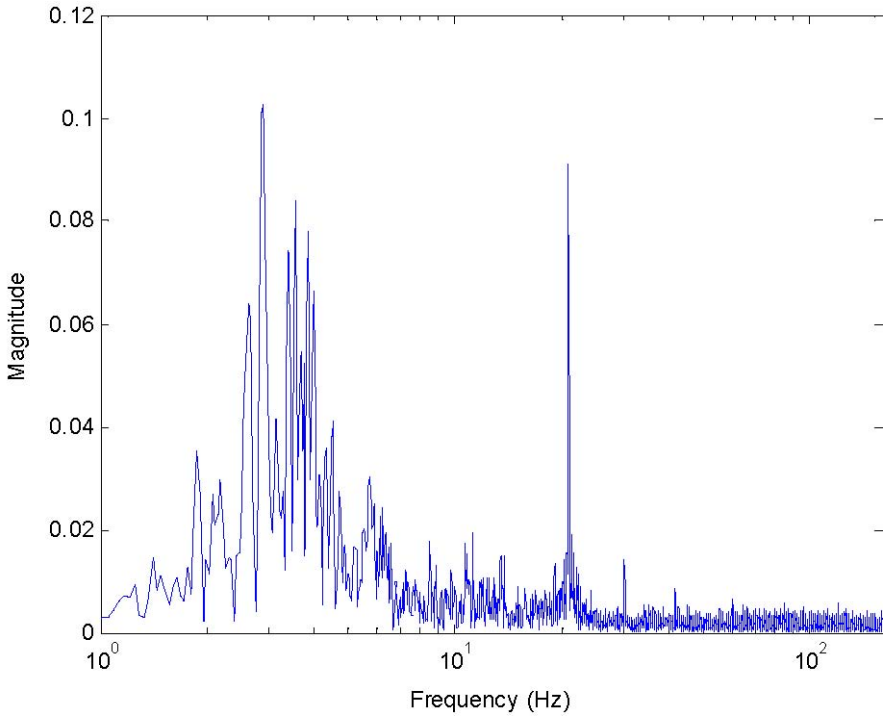

Figure 5. Frequency content of the passive energy at the Williams Street Park site

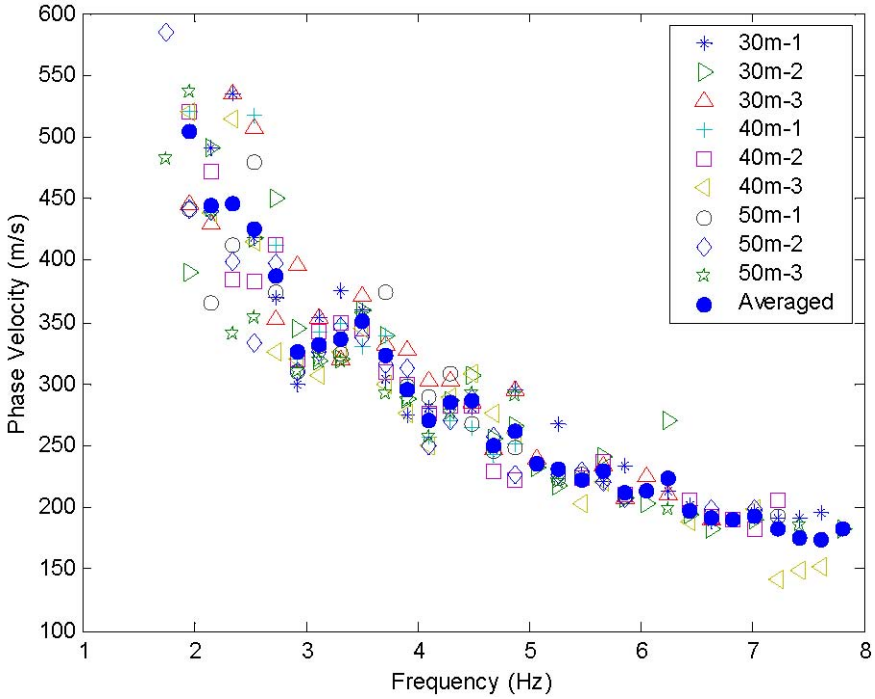

Figure 6. Experimental dispersion curves at Williams Street Park site (Passive tests)

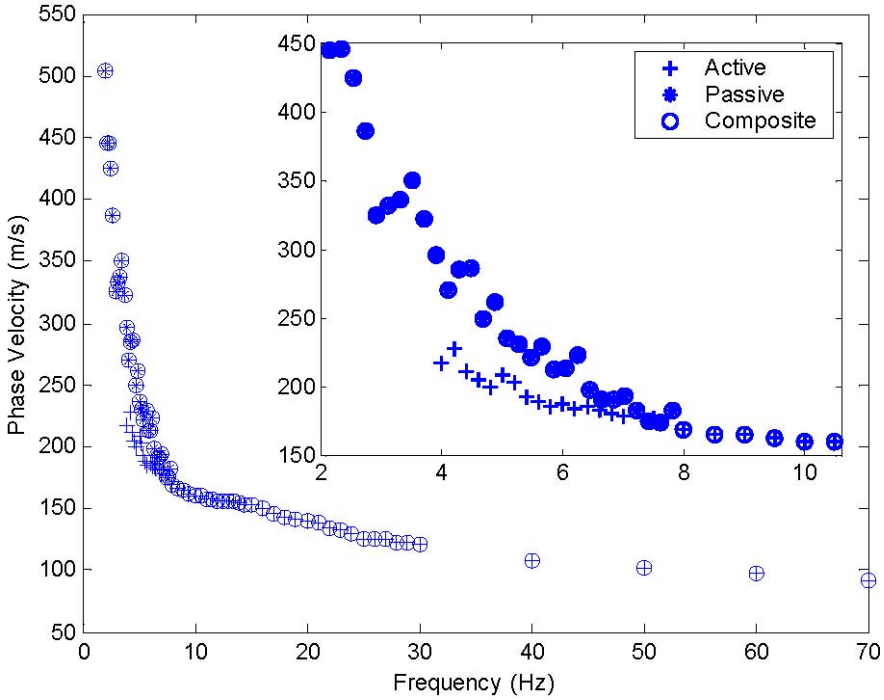

Figure 7. Experimental dispersion curve at the Williams Street Park site (Combined active-passive tests)

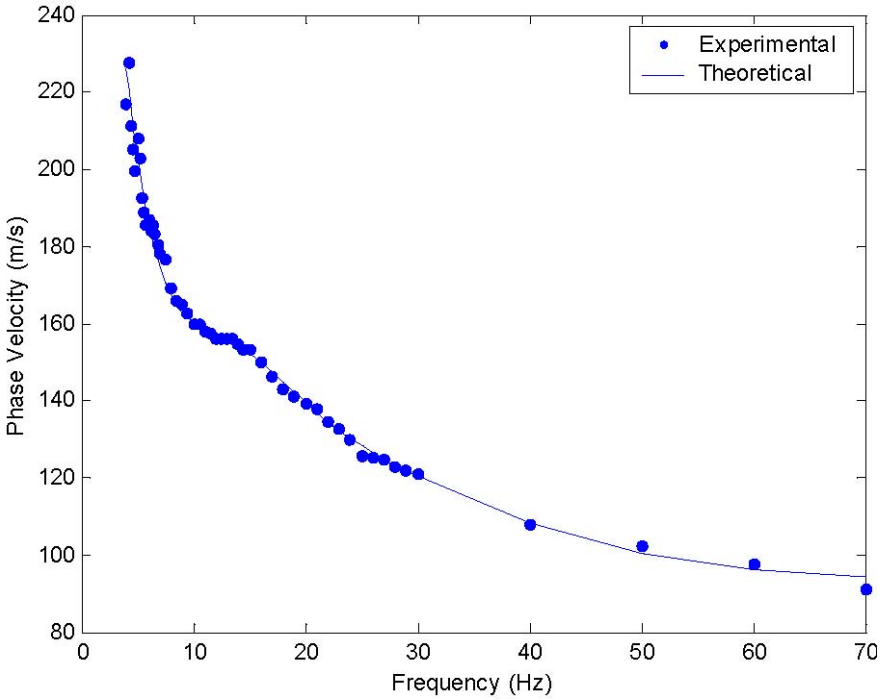

Figure 8. Comparison of experimental and theoretical dispersion curves at the Williams Street Park site (Active test)

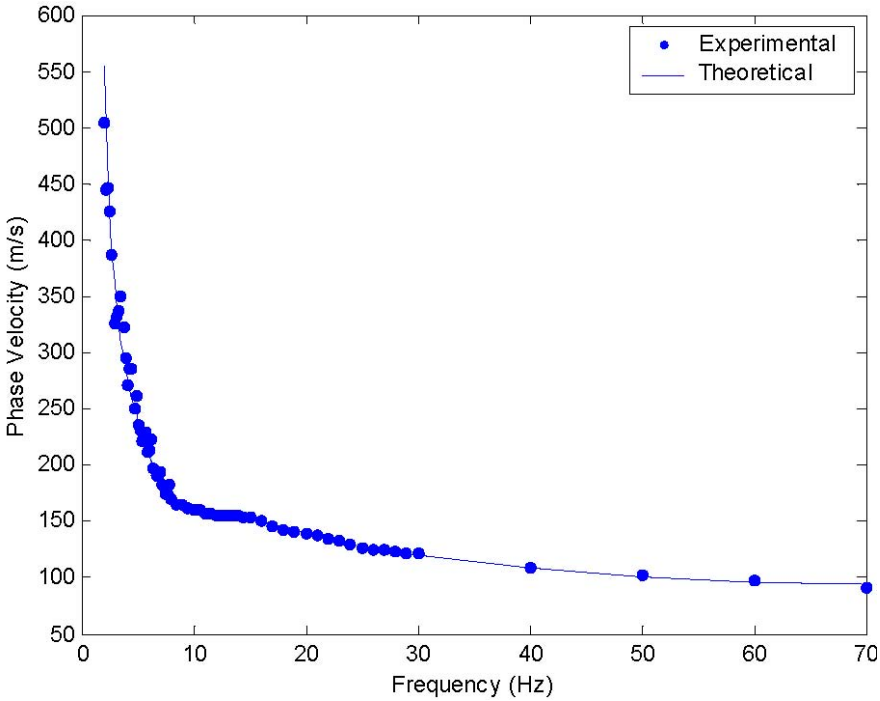

Figure 9. Comparison of experimental and theoretical dispersion curves at the Williams Street Park site (Combined active-passive tests)

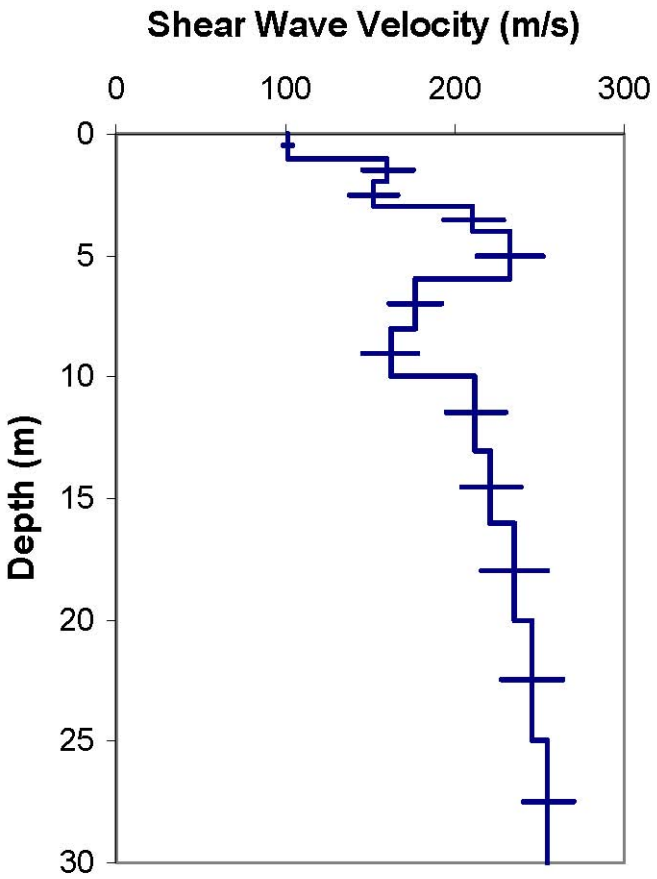

Figure 10. Shear wave velocity profile at the Williams Street Park site (Active test)

Table 1. Shear wave velocity profile and $\overline{V}_S$ at the Williams Street Park site (Active test)

Layer Thickness (m)	**Shear Wave Velocity (m/s)**	**Estimated Uncertainty (m/s)**
1	101	5.5
1	160	29.9
1	152	27.8
1	211	35.5
2	233	39.1
2	177	31.0
2	162	33.0
3	212	35.6
3	221	35.2
4	235	40.1
5	245	36.4
5	255	30.0
$\overline{V}_{S*}$	208	

* $\overline{V}_S$ is an average shear wave velocity in the upper 30 m.

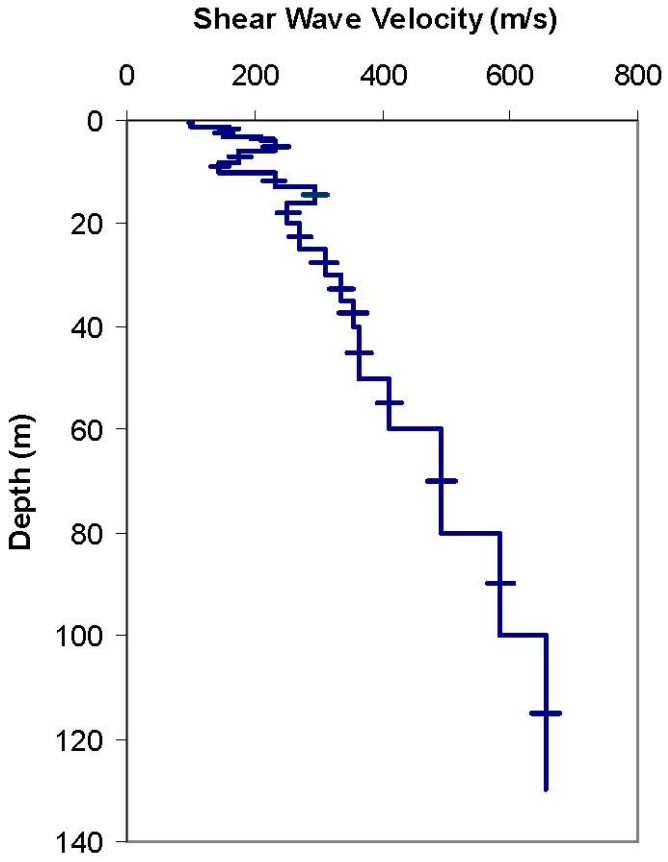

Figure 11. Shear wave velocity profile at the Williams Street Park site (Combined active-passive tests)

Table 2. Shear wave velocity profile and $\overline{V}_S$ at the Williams Street Park site (Combined active-passive tests)

Layer Thickness (m)	Shear Wave Velocity (m/s)	Estimated Uncertainty (m/s)
1	101	7.6
1	160	31.4
1	152	28.0
1	211	34.2
2	233	39.8
2	177	32.6
2	145	28.3
3	232	34.8
3	294	38.1
4	252	35.4
5	270	34.3
5	310	40.8
5	336	36.5
5	355	43.5
10	365	37.6
10	411	35.1
20	492	44.9
20	585	40.0
30	655	45.4
$\overline{V}_{S*}$	223	

* $\overline{V}_S$ is an average shear wave velocity in the upper 30 m.

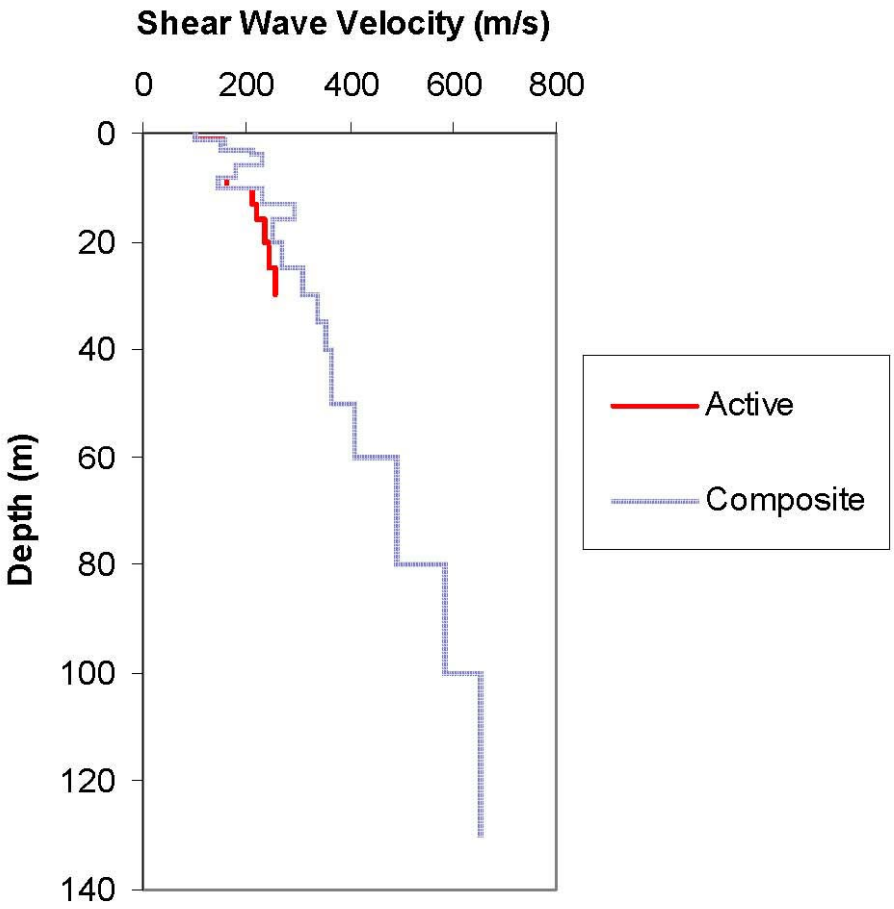

Figure 12. Comparison of shear wave velocity profiles at the Williams Street Park site.